JOURNAL OF BACTERIOLOGY, Apr. 2006, p. 2473–2482 Vol. 188, No. 7
0021-9193/06/$08.00+0 doi:10.1128/JB.188.7.2473–2482.2006

Mutations in DivL and CckA Rescue a *divJ* Null Mutant of *Caulobacter crescentus* by Reducing the Activity of CtrA

Deanne L. Pierce, Danielle S. O'Donnol,† Rebecca C. Allen, June W. Javens, Ellen M. Quardokus, and Yves V. Brun*

Department of Biology, Jordan Hall 142, Indiana University, 1001 E. 3rd Street, Bloomington, Indiana 47405

Received 16 September 2005/Accepted 10 January 2006

Polar development and cell division in *Caulobacter crescentus* are controlled and coordinated by multiple signal transduction proteins. *divJ* encodes a histidine kinase. A null mutation in *divJ* results in a reduced growth rate, cell filamentation, and mislocalized stalks. Suppressor analysis of *divJ* identified mutations in genes encoding the tyrosine kinase (*divL*) and the histidine kinase (*cckA*). The *divL* and *cckA* suppressor alleles all have single amino acid substitutions, some of which confer a temperature-sensitive phenotype, particularly in a wild-type background. Analysis of transcription levels from several positively regulated CtrA-dependent promoters reveals high expression in the *divJ* mutant, suggesting that DivJ normally serves to reduce CtrA activity. The *divL* and *cckA* suppressors reduce the amount of transcription from promoters positively regulated by CtrA, indicating that the mutations in *divL* and *cckA* are suppressing the defects of the *divJ* mutant by reducing the abnormally high level of CtrA activity. Immunoblotting showed no major perturbations in the CtrA protein level in any of these strains, suggesting that the high amount of CtrA activity seen in the *divJ* mutant and the reduced amount of activity in the suppressors are regulated at the level of activation and not transcription, translation, or degradation. In vivo phosphorylation assays confirmed that *divJ* mutants have elevated levels of CtrA phosphorylation and that this level is reduced in the suppressors with mutations in *divL*.

The aquatic gram-negative bacterium *Caulobacter crescentus* has a dimorphic life cycle, beginning as a motile, piliated swarmer cell incapable of DNA replication. The swarmer cell differentiates into a stalked cell by ejecting its flagellum, retracting the pili, and synthesizing a stalk with an adhesive holdfast at the same pole that contained the flagellum. The stalked cell initiates DNA replication and cell division and synthesizes a new flagellum at the pole opposite the stalk, producing a new motile swarmer cell during each cell cycle. Multiple signal transduction proteins are involved in coordinating polar development and cell division in *C. crescentus*. The global response regulator CtrA controls the expression of at least 144 genes (25) involved in cell division, DNA methylation, holdfast synthesis, flagellum biogenesis, and pilus biogenesis (22, 25, 34, 43). CtrA prevents the initiation of DNA replication in swarmer cells by binding to the origin of replication (35) and inhibits cell division by repressing transcription of *ftsZ*, which encodes the first cell division protein to localize to the site of division (22). Late in the cell cycle, CtrA activates transcription from the P_{QA} promoter, which cotranscribes *ftsQ* and *ftsA*, ensuring ordered expression of *ftsZ*, *ftsQ*, and *ftsA* (22, 38, 50).

CtrA activity is controlled by phosphorylation and proteolysis. CtrA is cleared from the swarmer cell during swarmer-to-stalked cell differentiation (9) in a ClpXP-dependent manner (21). Both CtrA and CtrA~P can be degraded by ClpXP (37), so dephosphorylation of CtrA during swarmer-to-stalked cell differentiation is not required for, nor is it likely to be the cue for, cell cycle-dependent proteolysis (37). DivK, an essential single-domain response regulator, plays a role in signaling the degradation of CtrA (16).

DivK is regulated by two histidine kinases, DivJ and PleC (15, 19, 51). *divJ* has been shown to be epistatic to *pleC* in terms of morphological phenotype (49). DivJ and PleC have antagonistic effects on DivK activity. DivJ localizes to the stalked pole of the cell, where it acts as a kinase for DivK, whereas PleC localizes to the flagellar pole and acts as a phosphatase, controlling the release of DivK from the pole (18, 49). The phosphorylation state of DivK controls its localization (24), causing it to shuttle between the flagellar pole and stalked pole in predivisional cells (28). Upon completion of cytokinesis, the shuttling ceases, and DivK no longer localizes to the flagellated pole, allowing development of the swarmer cell to occur (28). Thus, DivK is able to signal the state of cell compartmentalization during division (28). DivJ and PleC also have an antagonistic role on the GGDEF diguanylate cyclase response regulator PleD, which is involved in turning off flagellar rotation and in stalk synthesis (45). There is in vivo evidence that DivJ phosphorylates PleD, whereas PleC dephosphorylates PleD~P (3).

CtrA phosphorylation is controlled by DivL, an essential tyrosine kinase, and CckA, an essential hybrid kinase, which have the same localization pattern during the cell cycle (17, 18, 41, 52). DivL phosphorylates CtrA in vitro (52) and interacts with DivK, although the role of this interaction is not yet known (30). CckA is required for CtrA phosphorylation in vivo (17, 18), regulates the same subset of genes as CtrA, and is phosphorylated at the same time of the cell cycle as CtrA (17). CckA seems to have a stabilizing effect on the CtrA protein in addition to its putative role as a kinase for CtrA, as the half-life of CtrA decreases by over 50% in the absence of CckA (17). It remains to be seen whether both DivL and CckA are cognate

* Corresponding author. Mailing address: Indiana University, Department of Biology, 1001 E. 3rd Street, Bloomington, IN 47405. Phone: (812) 855-8860. Fax: (812) 855-6705. E-mail: ybrun@indiana.edu.

† Present address: Department of Mathematics, UCLA, Los Angeles, Calif.

TABLE 1. Strains and plasmids

Strain or plasmid	Description or construction	Source or reference(s)
Strains		
E. coli		
DH5αF′	ϕ80d*lacZ*ΔM15 Δ(*lacZYA-argF*)U169 *endA1 recA1 hsdR17*($r^- m^+$) *deoR thi-1 supE44* λ^- *gyrA96 relA1*	26
S17-1	*E. coli* 294::RP4-2(Tc::Mu)(Km::Tn*7*)	42
BL21(λDE3)	F^- *ompT hsdS*$_B$($r_B^- m_B^-$) *gal dcm* (λDE3)	Novagen
C. crescentus		
NA1000	*syn-1000*; previously called CB15N	12
CB15	CB15; wild type	31
CMS1–CMS40	Genomic marker strains; Kan^r	48
UJ590	CB15 ATCC 19089 Δ*pilA*	1
SU214	CB15N *rpoN*::Tn*5*	6
YB1382	CB15N *pleC*::mini-Tn*5 lacZ2* I29	13
YB3059	CB15 Δ*divJ*::*spec*	A. Hinz, unpublished
YB3202	NA1000 Δ*divJ*::*spec*	This study
YB1388	NA1000 *divJ*::mini-Tn*5 lacZ2*	This study
YB3215	NA1000 Δ*divJ*::*spec sdj-21* (original suppressor)	This study
YB3216	NA1000 Δ*divJ*::*spec sdj-22* (original suppressor)	This study
YB3219	NA1000 Δ*divJ*::*spec sdj-25* (original suppressor)	This study
YB3227	NA1000 Δ*divJ*::*spec sdj-33* (original suppressor)	This study
YB3229	NA1000 Δ*divJ*::*spec sdj-35* (original suppressor)	This study
YB3314	NA1000 *divL22* (exchanged suppressor)	This study
YB3315	NA1000 Δ*divJ*::*spec divL22* (exchanged suppressor)	This study
YB3316	NA1000 *divL33* (exchanged suppressor)	This study
YB3317	NA1000 Δ*divJ*::*spec divL33* (exchanged suppressor)	This study
YB3318	NA1000 *divL35* (exchanged suppressor)	This study
YB3319	NA1000 Δ*divJ*::*spec divL35* (exchanged suppressor)	This study
YB3325	NA1000 *cckA21* (exchanged suppressor)	This study
YB3326	NA1000 Δ*divJ*::*spec cckA21* (exchanged suppressor)	This study
YB3327	NA1000 *cckA25* (exchanged suppressor)	This study
YB3328	NA1000 Δ*divJ*::*spec cckA25* (exchanged suppressor)	This study
Plasmids		
pNPTS138	Used for two-part selection for in-frame deletions	4, 46
pHP45Ω	Used to obtain Ω cassette for spectinomycin resistance	32
pBGST18	Used to construct markers	4
pGSZ	Used to construct markers, a $Gent^r$ derivative of pGMTZ1	5
pJS70	Used to measure P*pilA* activity	43
plac290/HB2.0BP	Used to measure P*ftsZ* activity	22
pMSP8LC	Used to measure P*ftsQA* activity	38
pMR20	Medium-copy Tet^r plasmid	36
pJW375	Used to overexpress $DivL^{299}$	52
pNPTS138UP, DN, Ω	Used to delete *divJ*	This study
pMR20*divJ*	Used to complement *divJ* null mutants	This study
pBGST18CMS12.3	Used to generate genomic marker 3/10 of the way between CMS12 and CMS13	This study
pBGST18CMS12.4	Used to generate genomic marker 4/10 of the way between CMS12 and CMS13	This study
pBGST18CMS12.49	Used to generate genomic marker 49/100 of the way between CMS12 and CMS13	This study
pBGST18CMS12.54	Used to generate genomic marker 54/100 of the way between CMS12 and CMS13	This study
pBGST18CMS12.59	Used to generate genomic marker 59/100 of the way between CMS12 and CMS13	This study
pBGST18CMS12.6	Used to generate genomic marker 6/10 of the way between CMS12 and CMS13	This study
pBGST18CMS37.65	Used to generate genomic marker 65/100 of the way between CMS37 and CMS38	This study
pBGST18CMS37.75	Used to generate genomic marker 75/100 of the way between CMS37 and CMS38	J. Wagner, unpublished
pGSZCMS12.3	Used to generate genomic marker 3/10 of the way between CMS12 and CMS13	This study
pGSZCMS37.65	Used to generate genomic marker 65/100 of the way between CMS37 and CMS38	This study

kinases for CtrA or whether one or both are involved in a different stage of the pathway leading to the activation of CtrA.

CtrA activity controls so many cell cycle events, including cell division and DNA replication, that regulation of the level of CtrA activity is critical for optimal growth. In this paper, we show that *divJ* mutants have mislocalized holdfasts in addition to the mislocalized stalks, slow growth, and cell division defects previously described (40, 49). We use suppressor analysis to show that the defects of a *divJ* null mutant are due, at least in part, to increased CtrA activity. We provide in vivo evidence that DivJ normally acts to lower the activity of CtrA; therefore, mutations in *divL* and *cckA* suppress the *divJ* deletion mutant because they also lower the activity of CtrA.

MATERIALS AND METHODS

Bacterial strains, plasmids, and growth conditions. The bacterial strains and plasmids used in this study are described in Table 1. *Escherichia coli* strains were grown in Luria-Bertani (LB) broth or on LB agar (39) supplemented with kanamycin (30 μg/ml in broth, 50 μg/ml in agar), streptomycin (5 μg/ml in broth and agar), spectinomycin (100 μg/ml in broth, 50 μg/ml in agar), gentamicin (15

μg/ml in broth, 20 μg/ml in agar), and tetracycline (12 μg/ml in broth and agar) as necessary. *C. crescentus* strains were grown in peptone-yeast extract (PYE) broth or on PYE agar (31) supplemented with kanamycin (5 μg/ml in broth, 20 μg/ml in agar), spectinomycin (25 μg/ml in broth, 100 μg/ml in agar), gentamicin (2.5 μg/ml in agar), nalidixic acid (20 μg/ml in agar), tetracycline (1 μg/ml in broth, 2 μg/ml in agar), and 3% sucrose (in agar) as needed. *C. crescentus* strains transduced with Δ*divJ*::*spec* were grown on M2G agar (10) supplemented with spectinomycin (350 μg/ml) or kanamycin (100 μg/ml).

Two-step gene replacement or deletion. Two 450-bp fragments (UP and DN) on either side of *divJ* were amplified by PCR using oligonucleotides UPdivJN (5′-GTGGCGTATGCTAGCTACTGGGGG), UPdivJB (5′-GGGGAGGATG GATCCCGTCAAACC), DNdivJB (5′-TTTGCGCCGGGATCCGGCGCTCTG), and DNdivJH (5′-GCCTGTCGCAAAGCTTGAGCTTTGGG) and cloned into the vector pNPTS138 (4), along with a spectinomycin/streptomycin-resistant omega cassette (Ω) (32), to generate plasmid pNPTS138 UP, DN, Ω. The in-frame deletion was created by a two-step selection using the *nptI* gene to select for presence of the plasmid and the *sacB* and spectinomycin resistance genes to select against presence of the plasmid but for the presence of the Ω cassette, respectively (13, 47), to create YB3202 (Δ*divJ*::*spec*). The same technique was used to exchange the mutant alleles from *sdj-22*, *sdj-33*, *sdj-35*, *sdj-21*, and *sdj-25*, except that the entire gene was amplified and the Ω cassette was not used. The exchanges were confirmed by sequencing.

Complementation of *divJ* mutants. *divJ* and its presumptive promoter region were amplified by PCR using oligonucleotides divJUP and divJDN and cloned into the multicopy vector pMR20 (36), generating plasmid pMR20*divJ*.

Phage sensitivity assays. Two hundred microliters of saturated culture grown overnight was mixed with 3 ml of molten PYE–0.5% top agar and plated onto plain PYE plates. Once the top agar had hardened, 5 μl of 10^{10} PFU/ml φCr30 (11) and φCbK (2) was spotted onto each plate and allowed to soak in. The plates were incubated at 30°C for 3 days. NA1000 was used as a positive (sensitive) control, UJ590 (CB15 ATCC 19089 Δ*pilA*), a pilus-minus mutant, was used as a negative (resistant) control for φCbK, and YB1382 (CB15N *pleC*I29) was used as a negative (resistant) control for both phages. For a more quantitative measure of phage sensitivity, approximately 170 PFU of φCr30 were mixed with 3 ml PYE–0.5% top agar and 200 μl of culture grown overnight and plated onto a plain PYE plate and incubated at room temperature for 3 to 5 days.

Swarm motility assay. Five microliters of saturated cultures grown overnight or exponentially growing cells normalized to the same optical density at 600 nm (OD_{600}) was injected into fresh PYE–0.3% swarm agar plates. The plates were incubated at room temperature in a humid chamber for 5 days. NA1000 was used as a positive control, and SU214 (CB15N *rpoN*::Tn*5*) (6), a flagellum-minus mutant, was used as a negative control.

Transductions. Phage lysates were prepared as described previously (11). All transductions were done using a modification of the protocol described previously by West et al. (48). Briefly, 475 μl of culture grown overnight, 500 μl of PYE, and 25 μl of an irradiated phage lysate were mixed together. The mixture was incubated with shaking at 30°C for 1 to 4 h. Various amounts of the reaction mixture were plated onto PYE or M2G with appropriate antibiotics. φCr30 packages approximately 120 kb of DNA (*L*) (11), so if *d* is the distance between the gene and marker, and CTF is the cotransduction frequency, then CTF = $[1 - (d/L)]^3$. For example, the distance between *divL* and CMS38 is about 30 kb, so the expected CTF is 42%. Markers with decimal numbers were generated in this study and located between markers previously described (48). For example, marker CMS37.65 lies 65/100 of the way between markers CMS37 and CMS38. For three-factor crosses, the phage was grown on a doubly marked donor strain.

Mapping the suppressor mutations. We used transduction of markers spaced approximately 100 kb apart in the *C. crescentus* genome to map the locations of the suppressor mutations by transduction (48). The markers are numbered according to their location in the genome; for example, marker CMS37 is integrated at the 3.7-Mb position in the *C. crescentus* genome. We began by testing whether the suppressor mutations were linked to genes already known to be involved in developmental control, since it was likely that some of the suppressors of the *divJ* mutation would be in these genes. We identified markers linked to the wild-type allele of the suppressor mutation based on the ability of phage grown on a marked wild-type donor to transduce the suppressor strain back to the slow-growth phenotype of YB3202 (Δ*divJ*::*spec*). The expected CTFs of each marker with each gene of interest were estimated based on the distance between the gene and the site at which the marker was integrated. By comparing experimental CTFs with expected CTFs, we identified candidate genes for sequencing to identify the suppressor mutants.

Three suppressor mutants, *sdj-22*, *sdj-33*, and *sdj-35*, were linked to CMS38 with an average CTF of 23%. These suppressors were also 14% linked to CMS37. The suppressors showed a very strong linkage (69%) to CMS37.75, which is placed at 75% of the distance between CMS37 and CMS38. We reasoned that possible sites for suppressors of *divJ* could be located in *divL* at 37.70, CC3474 (*hk4*) at 37.62, and CC3477 (*rr4*) at 37.64. *hk4* (CC3474) and *rr4* (CC3477) were identified as cell cycle-regulated signal transduction genes (25). Another marker, CMS37.65, was constructed (with gentamicin resistance) and used in combination with CMS38 for three-factor crosses for *sdj-22*, *sdj-33*, and *sdj-35* to narrow the region to sequence for the suppressor mutation. The data for the three-factor cross indicated that the suppressor mutation mapped between CMS37.65 and CMS38, which ruled out *hk4* and *rr4* as possible sites for the mutation (data not shown).

Two suppressor mutants, *sdj-21* and *sdj-25*, were cotransduced 23% and 20%, respectively, with marker CMS12. This marker is near *divJ*, *cckN*, and *cckA*. Because the CMS12 marker is within cotransduction distance of *divJ*, donor lysates for subsequent mapping within cotransduction distance of *divJ* were made from a Δ*divJ*::*spec* background to avoid transducing the wild-type *divJ* allele along with the suppressor mutations. The *sdj-21* and *sdj-25* suppressor mutations were linked to CMS13 at 21% and 41%, respectively. This suggested that the mutation was between markers 12 and 13. Further mapping indicated that *sdj-21* was 53% linked and *sdj-25* was 58% linked to CMS12.6. A three-factor cross between a $Gent^r$ marker at position 12.3 and a Kan^r marker at position 12.6 showed that the suppressor mutations in *sdj-21* and in *sdj-25* lay between CMS12.3 and 12.6. Kan^r markers CMS12.4, 12.49, 12.54, and 12.59 were used to map the mutations more precisely. The suppressor mutants showed the greatest linkage to markers CMS12.49 and 12.54. *sdj-21* was shown to be 80% and 87% linked to CMS12.49 and CMS12.54, respectively, while *sdj-25* was 82% and 89% linked to the same markers, suggesting that the suppressor mutations were in *cckA*.

Sequencing. *divL* and the presumptive promoter region (573 bp upstream from the start of *divL*) were amplified as two fragments by PCR using oligonucleotide pairs divLF1 and R4 and divLF3 and R1. Additional oligonucleotides (divLF2-6 and divLR2-6) were designed approximately 550 bp apart for sequencing of the resultant PCR product. Oligonucleotides cckAF1 and cckAR1 were used to amplify *cckA* and the presumptive promoter region (422 bp upstream from the start site of *cckA*). Oligonucleotides cckAF2-F5 and cckAR2-R6 were used to sequence the resultant PCR product with cckAF1 and cckAR1. Sequencing reactions were performed using the ABI Prism BigDye Terminator cycle sequencing ready reaction kit (Applied Biosystems). Sequencing was performed by the Institute for Molecular and Cellular Biology at Indiana University on an Applied Biosystems 3730 automated fluorescence sequencing system. Wisconsin Package version 10.3 (Accelrys Inc.) and Sequencher 4.2.2 (Gene Codes Corporation) were used to analyze sequence data. All oligonucleotide sequences are available upon request.

DivL antibody production, immunoblot analysis, and β-galactosidase assays. Antibodies to DivL were generated by overexpressing the C-terminal 299 amino acids of DivL with a His tag from pJW375 (52) in BL21(λDE3) (Novagen) at 37°C in the presence of 1 mM IPTG (isopropyl-β-D-thiogalactopyranoside). The protein was purified from inclusion bodies as described previously (33). Polyclonal antibodies were raised in New Zealand White rabbits by Cocalico Biologicals (Reamstown, PA), and antibody was affinity purified as previously described (8).

Strains were grown to exponential phase (approximate OD_{600} of 0.6). From each culture, samples were removed for Lowry protein assay, Laemmli sodium dodecyl sulfate (SDS)-polyacrylamide gel electrophoresis, and β-galactosidase assays (23, 27, 29). Equal amounts of total protein were resolved on SDS-polyacrylamide gels and transferred onto nitrocellulose. After staining with Ponceau-S to confirm even transfer (14), the blots were probed with affinity-purified anti-DivL antibody at a dilution of 1:500 and anti-CtrA crude serum at a dilution of 1:700 overnight and treated with goat anti-rabbit immunoglobulin G (heavy plus light chains)–horseradish peroxidase conjugate (Bio-Rad) at a dilution of 1:20,000. The DivL blots were developed with Pierce SuperSignal West Dura substrate, and the CtrA blots were developed with Pierce SuperSignal Pico substrate. All blots were analyzed using a Kodak Image Station 440CF and Kodak 1D software.

Temperature-sensitive (TS) assays. Cultures of exponentially growing cells were diluted to an OD_{600} of 0.43, and 5 μl of 10^0, 10^{-2}, and 10^{-5} dilutions was spotted onto three sets of plain PYE plates (only one set is shown). The plates were incubated at 30°C, 34°C, and 37°C for 2 days and scanned. For microscopy, cultures were grown overnight in PYE at 30°C, subcultured into two new cultures, and allowed to grow to exponential phase at 30°C, and one culture was then shifted to 37°C and one was left at 30°C for 4 h (approximately 2.5 doublings at 30°C).

Microscopy. All images were captured using a Nikon Eclipse E800 with a Plan Apo ×100 oil immersion objective along with Princeton Instruments cooled charge-coupled-device digital camera model 1317 and MetaMorph imaging software (Universal Imaging Corporation). Lectin binding assays were performed as previously described (20), and fluorescence was observed using a Nikon FITC-HyQ filter cube (Chroma Technologies).

In vivo phosphorylation. In vivo phosphorylation was carried out as described previously (19), with the following modifications. Cells were grown in M5GG

TABLE 2. Phenotypes of the *divJ* suppressors

Strain	Locus	Avg cell length (μm) (no. of cells counted)	% of cells with stalks	Avg stalk length (μm) (no. of stalks counted)	φCbK	φCr30	Swarm motility
NA1000	NA[a]	3.03 (200)	67	1.48 (133)	S[b]	S	wt
YB3202 (Δ*divJ*::*spec*)	NA	3.97 (200)	64	3.00 (127)	S	S	*divJ*[e]
YB3215 (Δ*divJ*::*spec sdj-21*)	*cckA*	4.02 (192)	27	2.19 (51)	S	PS[c]	*divJ*[e]
YB3219 (Δ*divJ*::*spec sdj-25*)	*cckA*	3.12 (240)	13	1.81 (30)	S	PS	*divJ*[e]
YB3216 (Δ*divJ*::*spec sdj-22*)	*divL*	3.25 (141)	11	2.17 (16)	S	R[d]	*divJ*[e]
YB3227 (Δ*divJ*::*spec sdj-33*)	*divL*	3.47 (220)	11	1.61 (23)	S	R	*divJ*[e]
YB3229 (Δ*divJ*::*spec sdj-35*)	*divL*	3.10 (240)	13	1.95 (31)	S	R	*divJ*[e]

[a] NA, not applicable.
[b] S, sensitive.
[c] PS, partially sensitive.
[d] R, resistant.
[e] Less than the wild type (wt) and greater than a *fla* mutant.

medium to an OD_{600} of approximately 0.2. One milliliter of cells was removed for use in Western analysis. Five hundred microliters of cells was used for a Lowry protein assay. One milliliter of cells was washed with M5GG no-phosphate medium and labeled with 100 μCi [^{32}P]H_3PO_4 for 10 min. The pellet of labeled cells was resuspended in 50 μl SDS lysis buffer and frozen on dry ice. Ten microliters of RNaseA (10 mg/ml) was added, and the pellet was thawed for 2 min at room temperature. Six hundred fifty microliters of K2 low-salt buffer was added to the pellets. Three 100-μl aliquots of the lysate were used for the rest of the assay to assess reproducibility among individual immunoprecipitations. Thirty microliters of protein A agarose was added to the lysate along with 650 μl K2 low-salt buffer and incubated on a rocker at 4°C for 10 min. The protein A agarose was pelleted, and the supernatant was transferred to a new tube. CtrA was immunoprecipitated with 2 μl anti-CtrA crude serum and 20 μl protein A agarose for 30 min by rocking at 4°C. Washes and gel analysis were performed as described previously (19).

RESULTS

Analysis of *divJ* mutants. In a previous transposon mutagenesis screen for slow-growing mutants (13), we identified a mutant, called L35, that was deficient in cell division and exhibited a high frequency of stalk mislocalization. Sequencing of the *C. crescentus* DNA flanking the transposon revealed that the transposon was inserted after nucleotide 1018 of the *divJ* coding region, truncating the normally 597-amino-acid protein to 339 amino acids. This *divJ*::mini-Tn*5 lacZ2* mutant (YB1388) had characteristics similar to those of the previously reported *divJ* partial deletion mutant (49), but they differed in some respects. For example, more than 30% of cells of the partial *divJ* deletion mutant had misplaced stalks (49), compared to only 9% in our *divJ*::mini-Tn*5 lacZ2* mutant cells and 0.2% in wild-type NA1000. Because the previously reported *divJ* mutant was not a deletion of the entire gene, the differences between our *divJ*::mini-Tn*5 lacZ2* mutant and the previous *divJ* mutant could be due to the remaining *divJ* sequences in either or both mutants. We therefore constructed a *divJ* null mutant, replacing the entire coding sequence with the Ω cassette carrying spectinomycin resistance, resulting in YB3202 (Δ*divJ*::*spec*). The phenotype of the Δ*divJ*::*spec* mutant was complemented by plasmid pMR20*divJ* containing *divJ* under the control of its own promoter.

We analyzed the phenotype of YB3202 (Δ*divJ*::*spec*) by examining the length of the cells and stalks, the ability to swim in liquid and swarm in low-concentration agar, and sensitivity to phage (Table 2). YB3202 (Δ*divJ*::*spec*) had an average of 8% mislocalized stalks, compared to 9% mislocalized stalks in YB1388 (*divJ*::mini-Tn*5 lacZ2*) and 0.2% mislocalized stalks in NA1000. YB3202 (Δ*divJ*::*spec*) cells in a mixed population were approximately 4 μm long, compared to a 3-μm average length for NA1000 cells. The average length of stalks in YB3202 (Δ*divJ*::*spec*) was 3 μm, twice as long as stalks of NA1000 cells (Table 2). The Δ*divJ*::*spec* mutation was transduced into the CB15 background, creating YB3059 (CB15 Δ*divJ*::*spec*), to assay for the presence and location of holdfasts. YB3059 (CB15 Δ*divJ*::*spec*) produced holdfasts at the tips of polar stalks and at the tips of mislocalized side stalks (Fig. 1), suggesting that the Δ*divJ*::*spec* mutant has a general defect in cell polarity and not simply a defect in stalk localization. We saw no obvious differences in the swimming ability of swarmer cells of YB3202 (Δ*divJ*::*spec*) compared to that of cells of NA1000 by phase-contrast microscopy, but we found that YB3202 (Δ*divJ*::*spec*) does not form as large a swarm in 0.3% swarm agar as NA1000, as previously reported (Table 2) (7, 44). Since the defect in swarming is not due to an obvious defect in swimming, it is likely that the filamentous cells and the slow growth of the mutant are responsible for the swarming defect. We also examined the sensitivity of YB3202 (Δ*divJ*::*spec*) to the pilus-

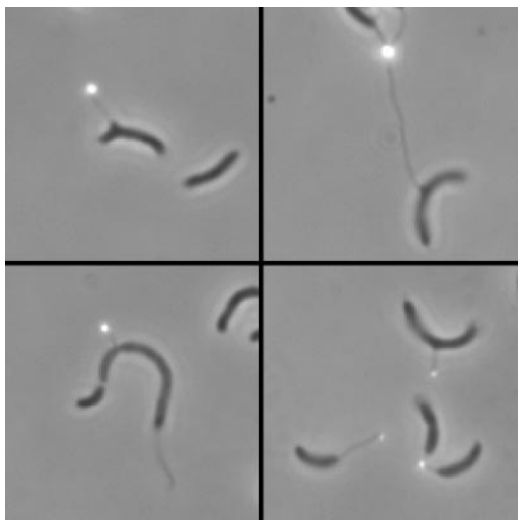

FIG. 1. Presence of holdfasts on mislocalized side stalks of YB3059 (CB15 Δ*divJ*::*spec*). Holdfasts were labeled with wheat germ agglutinin-fluorescein isothiocyanate and appear as white dots.

TABLE 3. Doubling times of the *divJ* and *sdj* mutants

Strain	Doubling time (min) ± SD
NA1000	94.1 ± 1.5
YB3202 (Δ*divJ*::*spec*)	103.5 ± 3.1
YB3326 (Δ*divJ*::*spec cckA21*)	96.3 ± 0
YB3328 (Δ*divJ*::*spec cckA25*)	97.6 ± 1.4
YB3315 (Δ*divJ*::*spec divL22*)	99.0 ± 0
YB3317 (Δ*divJ*::*spec divL33*)	98.1 ± 0.8
YB3319 (Δ*divJ*::*spec divL35*)	100.5 ± 0

specific phage φCbK and the S-layer phage φCr30. YB3202 was as sensitive to both phages as NA1000 (Table 2). In summary, YB3202 (Δ*divJ*::*spec*) is filamentous, has long, occasionally misplaced stalks, is deficient in swarming in 0.3% agar but not in swimming in liquid, and is sensitive to both S-layer and pilus-specific phage, and YB3059 (CB15 Δ*divJ*::*spec*) makes holdfast material associated with polar and misplaced stalks.

Isolation of fast-growing suppressors of a *divJ* null mutant. To determine the genetic basis for slow growth in the *divJ* mutant, we isolated suppressors of the slow-growth phenotype. Suppressors of the *divJ* mutation were obtained by repeatedly subculturing YB1388 or YB3202 (*divJ*::mini-Tn*5 lacZ2* or Δ*divJ*::*spec*) and plating aliquots daily. Fast-growing suppressors of the *divJ* mutant formed larger colonies than the original mutant, allowing for their easy identification (Table 3). As soon as a suppressor colony was identified from each of the independent cultures, no additional suppressors were isolated from that culture to avoid accumulation of multiple mutations in the same strain. The suppressors were named *sdj* mutants for *s*uppressor of *divJ*. Each of the suppressor mutants described in this study was isolated independently.

The first group of suppressor mutants, YB2761 to YB2763 and YB2766 to YB2768, was isolated from YB1388 (*divJ*::mini-Tn*5 lacZ2*), and the second group of suppressors, YB3215 to YB3229, was isolated from YB3202 (Δ*divJ*::*spec*). To eliminate any potential effects of the mini-Tn*5* in the suppressors isolated from YB1388 (*divJ*::mini-Tn*5 lacZ2*) and to facilitate mapping, we replaced the original *divJ*::mini-Tn*5 lacZ2* with Δ*divJ*::*spec* in the appropriate mutants by transduction, resulting in YB3203, YB3235, YB3236, and YB3238 to YB3240. The phenotypes of the transductants were indistinguishable from those of the original suppressors (data not shown).

Mutations in *divL* suppress the *divJ* phenotype. Mapping of the suppressor mutations in the *sdj-22*, *sdj-33*, and *sdj-35* suppressors indicated that they were closely linked to *divL* (see Materials and Methods). Sequencing confirmed the presence of single-base-change mutations in *divL* in the *sdj-22*, *sdj-33*, and *sdj-35* suppressors (Fig. 2A). In *sdj-22*, nucleotide 1259 of the coding sequence was changed from T to C, causing a V420A mutation in the DivL protein. In *sdj-33*, there was a T-to-G change at position 1560, corresponding to an F514V mutation in the protein. Finally, in *sdj-35*, nucleotide 1417 was changed from G to C, resulting in a G473R change in the protein. Each mutation was confirmed independently by PCR and sequencing. These mutations occur just upstream of the kinase domain of *divL*, possibly affecting phosphorylation activity.

We assayed each of the suppressors for several phenotypes (Table 2). *sdj-22*, *sdj-33*, and *sdj-35* were all more filamentous than the wild type but less filamentous than YB3202 (Δ*divJ*::*spec*). Fewer cells of *sdj-22*, *sdj-33*, and *sdj-35* had stalks than either NA1000 or YB3202 (Δ*divJ*::*spec*), and the length of the stalks was greater than NA1000 but less than YB3202 (Δ*divJ*::*spec*) (Table 2). *sdj-22*, *sdj-33*, and *sdj-35* were sensitive to φCbK but were resistant to φCr30. The resistance to φCr30 appeared to be a defect in supporting phage replication, as plaques were not formed, but cells were capable of being infected by phage, since they were able to be transduced. All three suppressors formed swarms similar in size to those of YB3202 (Δ*divJ*::*spec*) (Table 2). Because the suppressors were not significantly filamentous, their swarming deficiency cannot be due to a cell division defect as was the case for the Δ*divJ*::*spec* mutant. Microscopic examination of suppressor cultures revealed that the swarmer cells of these suppressors swam more slowly than the wild-type cells, which accounts for their small swarms in swarm agar.

We confirmed that each mutation in *divL* was solely responsible for the suppressor phenotype using allelic exchange. The *divL* alleles of each of the suppressors (*sdj-22*, *sdj-33*, and *sdj-35*) were exchanged in YB3202 (Δ*divJ*::*spec*). In each case, the *sdj* allele suppressed the *divJ* phenotype. Therefore, the *sdj-22*, *sdj-33*, and *sdj-35* alleles will hereafter be referred to as *divL22*, *divL33*, and *divL35*, respectively. The phenotypes of the allelic exchange mutants YB3315 (Δ*divJ*::*spec divL22*), YB3317 (Δ*divJ*::*spec divL33*), and YB3319 (Δ*divJ*::*spec divL35*) were identical to those of the original suppressor mutants described above.

We performed allelic exchange of the *divL* suppressor alleles in wild-type strain NA1000. The NA1000 *divL* strains YB3314 (NA1000 *divL22*), YB3316 (NA1000 *divL33*), and YB3318 (NA1000 *divL35*) formed small colonies compared to the wild type. This is especially interesting since, when combined with the Δ*divJ*::*spec* mutation, which also causes slow growth and small colonies, the double *divJ divL* mutants form large colonies and have growth rates similar to that of the wild type. The *sdj divL* alleles in the NA1000 background were also more filamentous than NA1000 and the Δ*divJ* mutant. The cells had stalk lengths that were approximately the same as those of wild-type cells. Many cells of the strains with *sdj divL* alleles in the NA1000 background had multiple constrictions. Levels of DivL protein were lower in YB3202 (the Δ*divJ*::*spec* mutant) but were at or slightly above wild-type levels in the suppressor

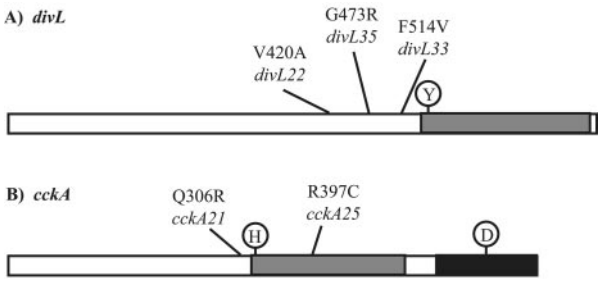

FIG. 2. Suppressor mutations mapping to *divL* and *cckA*. (A) Mutations in *divL*. Each mutation occurs only in the suppressor listed below it. The gray box represents the kinase domain, and Y is the catalytic tyrosine at position 550 in *divL*. (B) Mutations in *cckA*. Each mutation occurs only in the suppressor listed below it. The gray box represents the kinase domain, and H is the catalytic histidine at position 322 in *cckA*. The black box represents the *cckA* receiver domain, and D is the conserved aspartate at position 623.

TABLE 4. Relative levels of DivL and CtrA in the suppressors

Strain	DivL level (% of wt ± SD)[a]	CtrA level (% of wt ± SD)
NA1000	100	100
YB3202 (Δ*divJ*::*spec*)	64 ± 10	107 ± 10
YB3314 (*divJ*$^+$ *divL22*)	123 ± 40	100 ± 6
YB3315 (Δ*divJ*::*spec divL22*)	118 ± 32	116 ± 25
YB3316 (*divJ*$^+$ *divL33*)	112 ± 25	102 ± 19
YB3317 (Δ*divJ*::*spec divL33*)	110 ± 26	112 ± 23
YB3318 (*divJ*$^+$ *divL35*)	117 ± 26	87 ± 14
YB3319 (Δ*divJ*::*spec divL35*)	89 ± 17	85 ± 17

[a] wt, wild type.

mutants in both the NA1000 and YB3202 (Δ*divJ*::*spec*) backgrounds, as determined by immunoblot (Table 4).

The *divL* mutations confer TS lethality to wild-type cells and to a *divJ* null mutant. Because mutations in essential genes often result in a TS phenotype, and a previous *divL* mutant was TS (52), we examined the effects of temperature on the *divL sdj* alleles. All three NA1000 *sdj divL* strains were sensitive to 35°C and 37°C, whereas NA1000 and YB3202 (Δ*divJ*::*spec*) were not (Fig. 3). Two of the Δ*divJ*::*spec divL* strains, YB3315 (Δ*divJ*::*spec divL22*) and YB3317 (Δ*divJ*::*spec divL33*), also showed a sensitivity to temperatures above 30°C. The TS phenotype of *divL22* and *divL35* was weaker in the YB3202 (Δ*divJ*::*spec*) background than in the wild-type background (Fig. 3). YB3315 (Δ*divJ*::*spec divL22*) exhibited reduced growth at 37°C but not at 35°C. YB3317 (Δ*divJ*::*spec divL33*) was reduced for growth at both 35°C and 37°C, and YB3319 (Δ*divJ*::*spec divL35*) was not sensitive to either temperature (Fig. 3). To examine the morphology of the cells at permissive and nonpermissive temperatures, the NA1000 *divL* and Δ*divJ*::*spec divL* strains were grown to exponential phase in liquid culture at a permissive temperature (30°C) and shifted to a nonpermissive temperature (37°C) for 4 h. Five strains, YB3314 (NA1000 *divL22*), YB3315 (Δ*divJ*::*spec divL22*), YB3316 (NA1000 *divL33*), YB3317 (Δ*divJ*::*spec divL33*), and YB3318 (NA1000 *divL35*), became more filamentous after the incubation at 37°C, whereas NA1000, YB3202 (Δ*divJ*::*spec*), and YB3319 (Δ*divJ*::*spec divL35*) were not affected (Fig. 4). The most dramatic increase in cell length occurred in YB3316 (NA1000 *divL33*). The lack of increase in cell length in YB3319 (Δ*divJ*::*spec divL35*) correlates with the robust growth of this strain on plates at 37°C compared to the other strains (Fig. 3 and 4). The fact that the filamentous cells containing the *divL sdj* alleles had extended areas without constrictions suggests that the early stages of cell division are delayed in these mutants. The cells were also wider than in the YB3202 (Δ*divJ*::*spec*) background. Some cells of NA1000 *divL35* were bumpy (Fig. 4).

Mutations in *cckA* suppress the *divJ* phenotype. Mapping of the suppressor mutations in the *sdj-21* and *sdj-25* suppressors indicated that they were closely linked to *cckA* (see Materials and Methods). Sequencing confirmed the presence of single-base-change mutations in *cckA* in *sdj-21* and *sdj-25* (Fig. 2B). *sdj-21* had a mutation at nucleotide 917 of the coding sequence, with a G-to-A mutation causing a Q306R substitution. In *sdj-25*, the C at nucleotide 1189 was changed to a T, resulting in an R397C amino acid substitution. Each mutation was confirmed independently by PCR and sequencing. The *cckA* suppressor alleles (*sdj-21* and *sdj-25*) were exchanged with the wild-type allele in YB3202 (Δ*divJ*::*spec*). In both cases, the *sdj* allele suppressed the *divJ* mutant phenotype. The *sdj-21* and *sdj-25* mutations will hereafter be referred to as *cckA21* and *cckA25*, respectively. The phenotypes of the Δ*divJ*::*spec cckA* allelic exchange mutants, YB3326 (Δ*divJ*::*spec cckA21*) and YB3328 (Δ*divJ*::*spec cckA25*), were identical to those of the original suppressor mutants.

The *cckA21* and *cckA25* suppressors were different with respect to cell and stalk length (Table 2). The average cell length of the *cckA21* suppressor was similar to YB3202 (Δ*divJ*::*spec*), whereas the length of the *cckA25* suppressor was only slightly longer than NA1000. The *cckA21* suppressor had more cells with stalks than the *cckA25* strain, and the stalks were on average longer (Table 2). However, the *cckA21* suppressor and the *cckA25* suppressor were both sensitive to φCbK and partially sensitive to φCr30 and formed swarms similar in size to YB3202 (Δ*divJ*::*spec*) (Table 2). As with the suppressor mutants in *divL*, the suppressors in *cckA* also swam more slowly than the wild type, accounting for their small swarms in 0.3% swarm agar.

The *cckA21* and *cckA25* alleles were exchanged in NA1000, as described above. YB3325 (NA1000 *cckA21*) and YB3327 (NA1000 *cckA25*) formed smaller colonies than the wild type. YB3325 (NA1000 *cckA21*) was more filamentous than NA1000 and had longer stalks than NA1000 but had fewer of them. YB3327 (NA1000 *cckA25*) was also more filamentous than

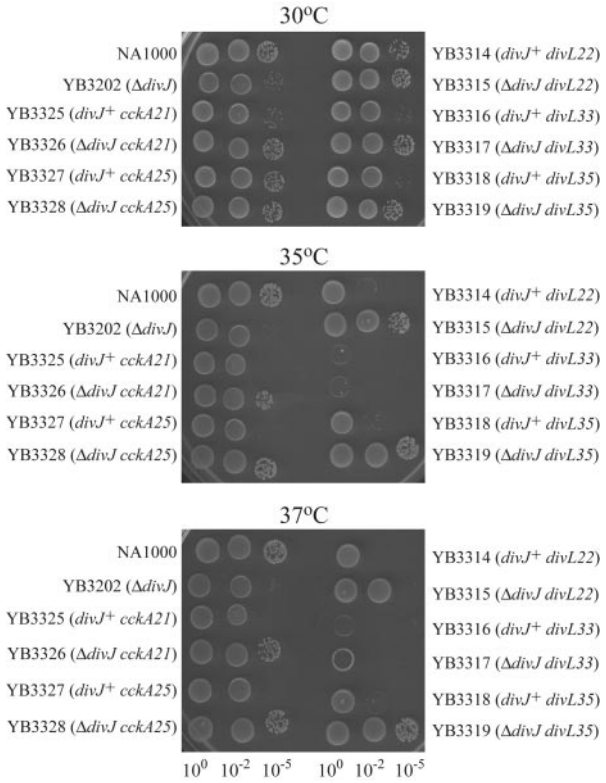

FIG. 3. Temperature sensitivity of *divJ* suppressors. Five microliters of exponential-phase cultures normalized to an OD_{600} of 0.43 and diluted as shown was spotted onto PYE plates in triplicate (only one set of plates is shown). Plates were incubated for 2 days at the indicated temperatures.

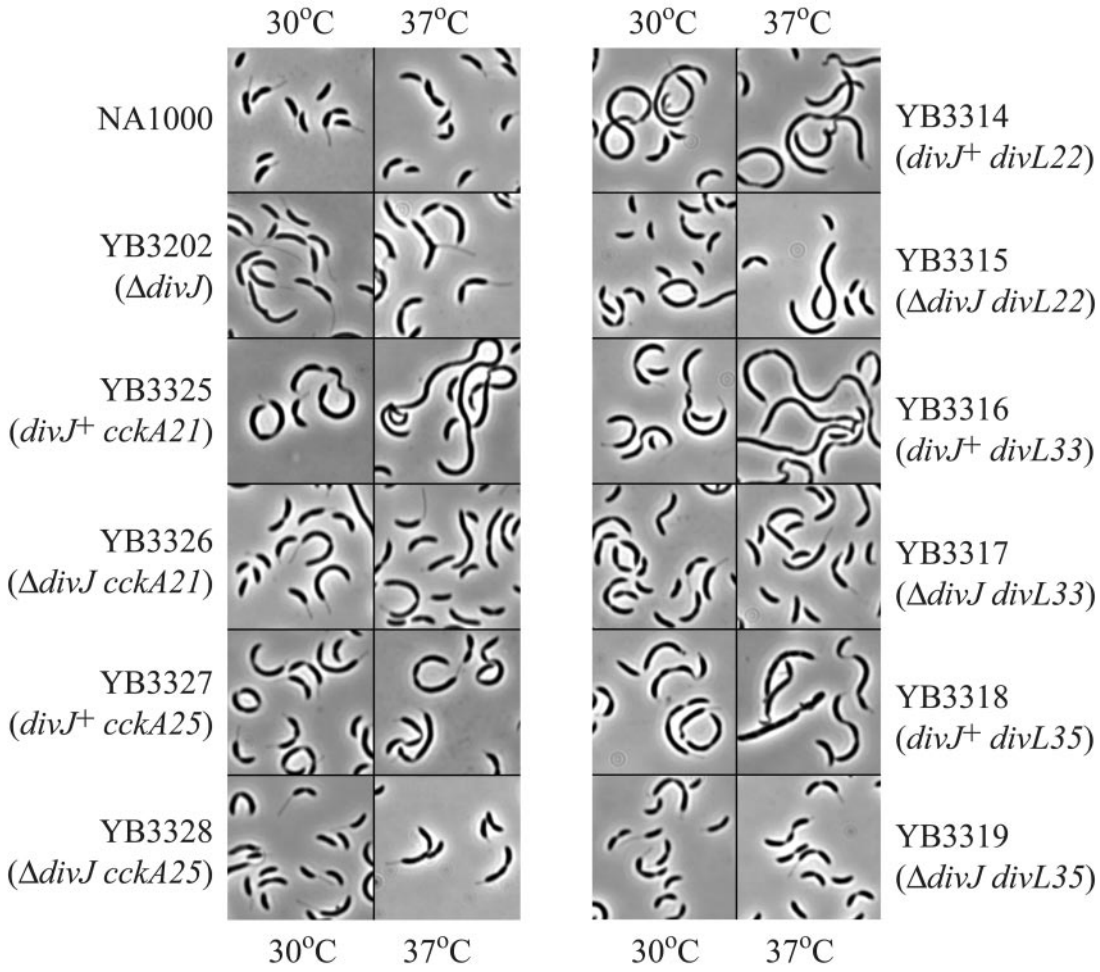

FIG. 4. Temperature-sensitive phenotypes of *divJ* suppressors. Phase-contrast micrographs show cells from exponentially growing cultures that were incubated at 30°C or 37°C for 4 h.

NA1000 but had approximately wild-type-length stalks, although it had fewer stalks than NA1000. There were multiple sites of constriction along the cells for both YB3325 (NA1000 *cckA21*) and YB3327 (NA1000 *cckA25*), but unlike the NA1000 *divL* strains, these cells were not bumpy. The NA1000 *cckA* strains, like the NA1000 *divL* strains, both formed small colonies compared to those formed by NA1000. As with the *divL* suppressor alleles, when the *cckA* suppressor alleles were combined with Δ*divJ*::*spec*, the two mutations, which independently cause small colonies and slow growth, restored wild-type colony size and growth.

The *cckA* mutations confer TS lethality to wild-type cells. Because *cckA* is essential, and a previous *cckA* mutant was TS, we examined the effects of temperature on the strains with the *cckA* alleles (Fig. 3). YB3325 (NA1000 *cckA21*) and YB3327 (NA1000 *cckA25*) exhibited reduced growth at 35°C and 37°C. Both strains were sensitive to temperatures of 35°C and 37°C, as seen for the 10^{-5} dilutions. However, the alleles in the YB3202 (Δ*divJ*::*spec*) background were virtually unaffected by temperatures above 30°C (Fig. 3). The growth of the spots of YB3326 (Δ*divJ*::*spec cckA21*) and YB3328 (Δ*divJ*::*spec cckA25*) was not reduced after incubation at 35°C and 37°C and was similar to the growth of spots grown at 30°C (Fig. 3). After exponentially growing cultures of YB3325 (NA1000 *cckA21*), YB3326 (Δ*divJ*::*spec cckA21*), YB3327 (NA1000 *cckA25*), and YB3328 (Δ*divJ*::*spec cckA25*) were shifted to 37°C for 4 h, YB3325 (NA1000 *cckA21*) had increased significantly in length, forming very long filaments with some areas of constriction, while YB3327 (NA1000 *cckA25*) had increased only slightly in length (Fig. 4). The filamentous cells of YB3325 (NA1000 *cckA21*) and YB3327 (NA1000 *cckA25*) with extended areas lacking constrictions suggest a delay in the early stages of cell division. Cells of the NA1000 *cckA* strains were also wider than wild-type cells. YB3326 (Δ*divJ*::*spec cckA21*) and YB3328 (Δ*divJ*::*spec cckA25*) only increased slightly in length, which correlates with the robust growth on plates at 35°C and 37°C (Fig. 3 and 4). NA1000 and YB3202 (Δ*divJ*::*spec*) were not affected (Fig. 4). The late-cell-division phenotype of both the *divL* and *cckA* suppressors led us to examine CtrA activity in the Δ*divJ* mutant and the suppressor mutants.

CtrA activity, but not protein level, is reduced in the *sdj* mutants. CtrA phosphorylation occurs late in the cell cycle and is required to activate transcription of cell division genes *ftsQ* and *ftsA*, which are needed to complete the division process (38, 50). Therefore, we hypothesized that the suppression of the *divJ* phenotype was due to a lowered CtrA activity. The

TABLE 5. Relative activity of the *pilA* promoter in the presence of *sdj* mutations

Strain	*pilA* transcription (% of wt ± SD)[a]
NA1000	100 ± 6.13
YB3202 (Δ*divJ*)	128 ± 6.37
YB3325 (*divJ*$^+$ *cckA21*)	34 ± 7.73
YB3326 (Δ*divJ*::*spec cckA21*)	66 ± 3.16
YB3327 (*divJ*$^+$ *cckA25*)	56 ± 4.80
YB3328 (Δ*divJ*::*spec cckA25*)	88 ± 4.35
YB3314 (*divJ*$^+$ *divL22*)	44 ± 5.02
YB3315 (Δ*divJ*::*spec divL22*)	52 ± 11.86
YB3316 (*divJ*$^+$ *divL33*)	46 ± 5.42
YB3317 (Δ*divJ*::*spec divL33*)	47 ± 9.13
YB3318 (*divJ*$^+$ *divL35*)	49 ± 12.79
YB3319 (Δ*divJ*::*spec divL35*)	64 ± 6.79

[a] Activity was measured as Miller units and then expressed as a percentage of the wild type (wt), with wild-type activity equal to 100%.

amount of CtrA, as determined by immunoblot, in the different suppressor mutants (in both the NA1000 and YB3202 [Δ*divJ*::*spec*] backgrounds) did not differ significantly (Table 4). We used *pilA-lacZ* fusions as a measure of CtrA activity level since the transcription of *pilA* depends on CtrA (43) (Table 5). *pilA-lacZ* transcription was higher in YB3202 (Δ*divJ*::*spec*) than in NA1000, suggesting that CtrA activity was higher in the Δ*divJ* mutant, since the CtrA concentration was the same as that in the wild type (Table 4). *pilA-lacZ* transcription was reduced in the *divL* and *cckA sdj* mutants, more so in the NA1000 background than in the YB3202 (Δ*divJ*::*spec*) background (Table 5). These results suggest that the phenotype of the Δ*divJ*::*spec* mutant is due at least in part to increased CtrA activity and that the *divL* and *cckA* alleles suppress those defects by reducing the activity of CtrA. Since CtrA regulates cell division, and because cells of the suppressor alleles in NA1000 have a late-cell-division phenotype, we next examined the transcription of genes encoding proteins involved in cell division.

***ftsZ* and *ftsQA* promoter activity is altered in the *divJ* mutant and in *divJ* suppressor strains.** The cell division phenotype of the *divJ* null mutant, with cells often containing extended regions without constrictions, suggested that the frequency of cell division initiation was reduced. This is consistent with our model that the *divJ* null mutant has an increased level of CtrA activity, since CtrA represses *ftsZ* transcription (22) and activates *ftsQA* transcription (50). *ftsZ* is required for the initiation of cell division, whereas *ftsQ* and *ftsA*, whose transcription is activated by CtrA, act later in cell division (38). We used β-galactosidase assays to examine the levels of transcription from the *ftsZ* and *ftsQA* promoters in the suppressor mutants along with NA1000 and YB3202 (Δ*divJ*::*spec*) (Table 6). As expected, transcription from the *ftsZ* promoter was only about 60% of that of the wild type in YB3202 (Δ*divJ*::*spec*). Conversely, *ftsQA* transcription was approximately 20% higher in YB3202 (Δ*divJ*::*spec*) than in the wild type. All five *sdj* mutants (in both the NA1000 and the Δ*divJ*::*spec* mutant backgrounds) had nearly wild-type levels of *ftsZ* transcription, while *ftsQA* transcription was at or below wild-type levels (Table 6). This was true for both the permissive temperature of 30°C and the nonpermissive temperature of 37°C. These results are consistent with the model that the *divJ* null mutant has an increased level of CtrA activity and that the *divL* and *cckA* alleles suppress the *divJ* phenotype by reducing CtrA activity.

CtrA phosphorylation is increased in Δ*divJ*::*spec* and reduced in an *sdj* mutant. Results from promoter analysis suggested that the Δ*divJ*::*spec* mutant has higher CtrA activity than wild-type cells and that the *sdj* mutations reduce CtrA activity. To directly test this possibility, we used in vivo phosphorylation assays. Cells were labeled with radioactive inorganic phosphate, followed by immunoprecipitation of CtrA and quantitation of the amount of CtrA~P by phosphorimaging. The CtrA~P values were normalized to the abundance of CtrA as determined by Western blot. The results in Fig. 5 show that the Δ*divJ*::*spec* mutant has a higher level of CtrA~P than wild-type cells. The presence of the *divL35* allele in both the NA1000 background and the Δ*divJ*::*spec* background (YB3318 and YB3319, respectively) reduced the amount of CtrA~P to below that of the wild type (Fig. 5). These results provide direct support for the model that the *divJ* null mutant phenotype is due, at least in part, to increased CtrA~P and that the *divL* alleles suppress the *divJ* null phenotype by reducing the amount of CtrA~P. Since the *cckA* alleles had effects on gene expression similar to those of the *divL* alleles and had similar

TABLE 6. *ftsZ* and *ftsQA* transcription in the presence of *sdj* mutations

Strain	Transcription level (% of wt ± SD)[a]			
	ftsZ		*ftsQA*	
	30°C	37°C	30°C	37°C
NA1000	100 ± 17.46	100 ± 7.68	100 ± 2.95	100 ± 3.44
YB3202 (Δ*divJ*)	64 ± 4.06	61 ± 9.48	127 ± 9.59	113 ± 5.03
YB3325 (*divJ*$^+$ *cckA21*)	96 ± 5.80	86 ± 6.03	67 ± 1.68	45 ± 1.17
YB3326 (Δ*divJ*::*spec cckA21*)	103 ± 6.00	101 ± 2.85	112 ± 2.75	115 ± 6.13
YB3327 (*divJ*$^+$ *cckA25*)	88 ± 4.49	92 ± 8.01	70 ± 1.60	54 ± 7.71
YB3328 (Δ*divJ*::*spec cckA25*)	84 ± 1.01	105 ± 2.80	101 ± 2.51	100 ± 5.12
YB3314 (*divJ*$^+$ *divL22*)	93 ± 2.05	85 ± 5.58	69 ± 4.14	41 ± 11.68
YB3315 (Δ*divJ*::*spec divL22*)	106 ± 3.91	130 ± 5.99	102 ± 1.09	96 ± 1.95
YB3316 (*divJ*$^+$ *divL33*)	92 ± 8.17	91 ± 7.82	96 ± 6.41	55 ± 24.36
YB3317 (Δ*divJ*::*spec divL33*)	108 ± 3.13	113 ± 4.75	97 ± 3.80	69 ± 19.14
YB3318 (*divJ*$^+$ *divL35*)	97 ± 5.49	93 ± 2.54	104 ± 7.50	91 ± 5.07
YB3319 (Δ*divJ*::*spec divL35*)	105 ± 11.67	119 ± 4.02	113 ± 22.68	112 ± 3.18

[a] Activity was measured as Miller units and then expressed as a percentage of the wild type (wt), with wild-type activity equal to 100%.

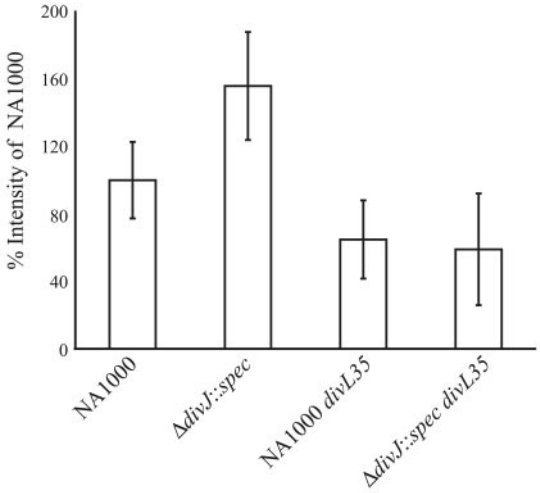

FIG. 5. Levels of CtrA~P relative to CtrA in the *divJ* null mutant and a *divJ* suppressor mutant (*divL35*). Data are averages of three independent experiments, each done in triplicate (nine samples total). The CtrA~P band intensity was divided by the CtrA band intensity based on loading equal total protein for the in vivo phosphorylation and Western blot.

cell division phenotypes, we hypothesize that they also suppress the *divJ* phenotype by the same mechanism.

DISCUSSION

DivJ is involved in the pathway controlling CtrA activity by controlling the level of DivK~P (15, 49), which in turn controls CtrA degradation (16). The kinase domain of DivJ can phosphorylate DivK in vitro (15), and the amount of DivK~P in vivo is reduced in a *divJ* null mutant (49). Additional evidence for DivJ acting upstream of CtrA comes from the ability of the *sokA* allele of *ctrA* to suppress the cell division phenotype of a *divJ* cold-sensitive mutant (51). In this paper, we describe a screen for suppressors of a *divJ* null mutant that provides in vivo evidence for the role of DivJ in controlling the activity of CtrA. Suppression of a *divJ* null mutant by alleles of *divL* and *cckA* appears to reduce CtrA activity without reducing the cellular level of CtrA. This strongly suggests that at least part of the defect of a *divJ* null mutant is due to increased CtrA activity. Indeed, DivL can phosphorylate CtrA in vitro (52), and CckA is required for CtrA phosphorylation in vivo (17, 18).

Since DivJ is responsible for the phosphorylation of DivK, eventually leading to the degradation of CtrA~P (16, 49), the excess active CtrA in the *divJ* mutant may be the result of inefficient degradation of CtrA~P. However, this is unlikely, since the cellular level of CtrA is not significantly reduced in the *divJ* null mutant compared to the wild type. Therefore, it appears that the defect of the *divJ* null mutant is due in part to an imbalance of CtrA~P compared to CtrA. The mutations in DivL and CckA are likely to be partial loss-of-function mutations, causing them to function less efficiently as kinases, leading to reduced CtrA~P. This is supported by the fact that these mutations lead to filamentation of cells when present in an otherwise-wild-type background; this is the phenotype of DivL and CckA loss-of-function mutants (18, 52). Alternatively, the mutations may cause an increase in the phosphatase activity of DivL and CckA, again resulting in reduced CtrA~P. Thus, the *sdj* mutations in DivL and CckA compensate for the lack of DivJ by causing a reduction in the levels of CtrA~P but not a reduction in the overall amount of CtrA. It should be noted that the suppression of the *divJ* null phenotype is not perfect with respect to stalk presence and length. This could be due to faulty regulation of PleD, which is normally phosphorylated by DivJ (3). PleD controls loss of motility and stalk formation at the swarmer-to-stalked cell transition (45).

We believe that the *divJ* phenotype (filamentous cells with long, sometimes misplaced stalks) is due in part to an abnormally high level of active CtrA, CtrA~P, in the cell. This phenotype is similar to that of *divK*(Cs) at nonpermissive temperatures (15), which results in an excess of CtrA activity as well, in this case by reducing CtrA degradation (16). The high levels of *pilA* transcription in the Δ*divJ* mutant compared to that in the wild type support our hypothesis, since *pilA* transcription is directly activated by CtrA~P (43). As we expected, the *divL* and *cckA* suppressor mutant alleles reduce *pilA* transcription in both the wild-type and YB3202 (Δ*divJ*::*spec*) backgrounds. The high level of *pilA-lacZ* transcription in YB3202 (Δ*divJ*::*spec*) and the reduced levels in the suppressor mutants suggest that the suppression occurs by reducing the amount of active CtrA (CtrA~P) in the cells and not by altering the cellular level of the protein. Indeed, there is an increase in the amount of CtrA~P in YB3202 (Δ*divJ*::*spec*) and a reduction of CtrA~P in YB3318 (NA1000 *divL35*) and YB3319 (NA1000 Δ*divJ*::*spec divL35*) compared to the wild-type.

The overabundance of active CtrA can also explain the cell division phenotype seen in the *divJ* null mutant. Active CtrA represses transcription of *ftsZ* and activates transcription of *ftsQ* and *ftsA* from the P_{QA} promoter (50). The Δ*divJ*::*spec* mutant has reduced *ftsZ* transcription and increased transcription of *ftsQA* compared to the wild type. Since FtsZ is required for the initiation of cell division (33), and increased FtsA expression inhibits cell division (38), the effect of the *divJ* mutation on *ftsZ* and *ftsQA* transcription is to reduce the frequency of cell division. The *divJ* suppressors are not as filamentous as the Δ*divJ*::*spec* mutant and grow at rate similar to that of the wild type, consistent with the fact that the *sdj* suppressors restore *ftsZ* and *ftsQA* expression to near-wild-type levels in the Δ*divJ*::*spec* background.

Another explanation for the high level of active CtrA in the Δ*divJ*::*spec* mutant is that DivJ may act as a phosphatase for CtrA~P, in addition to its role as a kinase for DivK and PleD. In a *divJ* null mutant, levels of CtrA~P would rise, resulting in the filamentous phenotype of the Δ*divJ*::*spec* mutant. Mutations in DivL and CckA that reduce their effectiveness in phosphorylating CtrA would compensate for the loss of DivJ phosphatase activity by reducing the amount of CtrA~P made in the first place.

In conclusion, our results support the hypothesis that the phenotype of *divJ* null mutants is the result of excess active CtrA. Mutations in DivL and CckA reduce the activity of these kinases in phosphorylating CtrA or increase their activity in dephosphorylating CtrA, thereby suppressing the loss of DivJ. Future work on the DivL mutant proteins will help determine the exact nature of this suppression.

ACKNOWLEDGMENTS

This work was supported by NIH predoctoral training grant GM07757 to D.L.P. and NIH grant GM51986 to Y.V.B.

We thank A. Newton for the DivL overexpression construct for antibody production, C. Stephens for marker strains, K. Ryan and C. Jacobs-Wagner for advice on in vivo phosphorylation, and members of our laboratory for helpful discussions and critical reading of the manuscript.

REFERENCES

1. **Ackermann, M., S. C. Stearns, and U. Jenal.** 2003. Senescence in a bacterium with asymmetric division. Science **300:**1920.
2. **Agabian-Keshishian, N., and L. Shapiro.** 1970. Stalked bacteria: properties of deoxyribonucleic acid bacteriophage ϕCBK. J. Virol. **5:**795–800.
3. **Aldridge, P., R. Paul, P. Goymer, P. Rainey, and U. Jenal.** 2003. Role of the GGDEF regulator PleD in polar development of *Caulobacter crescentus*. Mol. Microbiol. **47:**1695–1708.
4. **Alley, M. R. K.** Unpublished data.
5. **Alley, M. R. K., S. L. Gomes, W. Alexander, and L. Shapiro.** 1991. Genetic analysis of a temporally transcribed chemotaxis gene cluster in *Caulobacter crescentus*. Genetics **129:**333–342.
6. **Brun, Y. V., and L. Shapiro.** 1992. A temporally controlled sigma factor is required for cell-cycle dependent polar morphogenesis in *Caulobacter*. Genes Dev. **6:**2395–2408.
7. **Burton, G. J., G. B. Hecht, and A. Newton.** 1997. Roles of the histidine protein kinase PleC in *Caulobacter crescentus* motility and chemotaxis. J. Bacteriol. **179:**5849–5853.
8. **Din, N., E. M. Quardokus, M. J. Sackett, and Y. V. Brun.** 1998. Dominant C-terminal deletions of FtsZ that affect its ability to localize in *Caulobacter* and its interaction with FtsA. Mol. Microbiol. **27:**1051–1064.
9. **Domian, I. J., K. C. Quon, and L. Shapiro.** 1997. Cell type-specific phosphorylation and proteolysis of a transcriptional regulator controls the G1-to-S transition in a bacterial cell cycle. Cell **90:**415–424.
10. **Ely, B.** 1991. Genetics of *Caulobacter crescentus*. Methods Enzymol. **204:**372–384.
11. **Ely, B., and R. C. Johnson.** 1977. Generalized transduction in *Caulobacter crescentus*. Genetics **87:**391–399.
12. **Evinger, M., and N. Agabian.** 1977. Envelope-associated nucleoid from *Caulobacter crescentus* stalked and swarmer cells. J. Bacteriol. **132:**294–301.
13. **Gonin, M., E. M. Quardokus, D. O'Donnol, J. Maddock, and Y. V. Brun.** 2000. Regulation of stalk elongation by phosphate in *Caulobacter crescentus*. J. Bacteriol. **182:**337–347.
14. **Harlow, E., and D. Lane.** 1988. Antibodies: a laboratory manual. Cold Spring Harbor Laboratory Press, Plainview, N.Y.
15. **Hecht, G. B., T. Lane, N. Ohta, J. M. Sommer, and A. Newton.** 1995. An essential single domain response regulator required for normal cell division and differentiation in *Caulobacter crescentus*. EMBO J. **14:**3915–3924.
16. **Hung, D. Y., and L. Shapiro.** 2002. A signal transduction protein cues proteolytic events critical to Caulobacter cell cycle progression. Proc. Natl. Acad. Sci. USA **99:**13160–13165.
17. **Jacobs, C., N. Ausmees, S. J. Cordwell, L. Shapiro, and M. Laub.** 2003. Functions of the CckA histidine kinase in Caulobacter cell cycle control. Mol. Microbiol. **47:**1279–1290.
18. **Jacobs, C., I. J. Domian, J. R. Maddock, and L. Shapiro.** 1999. Cell cycle-dependent polar localization of an essential bacterial histidine kinase that controls DNA replication and cell division. Cell **97:**111–120.
19. **Jacobs, C., D. Hung, and L. Shapiro.** 2001. Dynamic localization of a cytoplasmic signal transduction response regulator controls morphogenesis during the Caulobacter cell cycle. Proc. Natl. Acad. Sci. USA **98:**4095–4100.
20. **Janakiraman, R. S., and Y. V. Brun.** 1999. Cell cycle control of a holdfast attachment gene in *Caulobacter*. J. Bacteriol. **181:**1118–1125.
21. **Jenal, U., and T. Fuchs.** 1998. An essential protease involved in bacterial cell-cycle control. EMBO J. **17:**5658–5669.
22. **Kelly, A. J., M. J. Sackett, N. Din, E. M. Quardokus, and Y. V. Brun.** 1998. Cell cycle-dependent transcriptional and proteolytic regulation of FtsZ in *Caulobacter*. Genes Dev. **12:**880–893.
23. **Laemmli, U. K.** 1970. Cleavage of structural proteins during the assembly of the head of bacteriophage T4. Nature **227:**680–685.
24. **Lam, H., J. Y. Matroule, and C. Jacobs-Wagner.** 2003. The asymmetric spatial distribution of bacterial signal transduction proteins coordinates cell cycle events. Dev. Cell **5:**149–159.
25. **Laub, M. T., S. L. Chen, L. Shapiro, and H. H. McAdams.** 2002. Genes directly controlled by CtrA, a master regulator of the *Caulobacter* cell cycle. Proc. Natl. Acad. Sci. USA **99:**4632–4637.
26. **Liss, L. R.** 1987. New M13 host: DH5αF′ competent cells. Focus **9:**3, 13.
27. **Lowry, O. H., N. R. Rosebrough, A. L. Farr, and R. J. Randall.** 1951. Protein measurement using the folin phenol reagent. J. Biol. Chem. **193:**265–275.
28. **Matroule, J. Y., H. Lam, D. T. Burnette, and C. Jacobs-Wagner.** 2004. Cytokinesis monitoring during development; rapid pole-to-pole shuttling of a signaling protein by localized kinase and phosphatase in *Caulobacter*. Cell **118:**579–590.
29. **Miller, J. H.** 1972. Experiments in molecular genetics. Cold Spring Harbor Laboratory, Cold Spring Harbor, N.Y.
30. **Ohta, N., and A. Newton.** 2003. The core dimerization domains of histidine kinases contain recognition specificity for the cognate response regulator. J. Bacteriol. **185:**4424–4431.
31. **Poindexter, J. S.** 1964. Biological properties and classification of the *Caulobacter* group. Bacteriol. Rev. **28:**231–295.
32. **Prentki, P., and H. M. Krisch.** 1984. *In vitro* insertional mutagenesis with a selectable DNA fragment. Gene **29:**303–313.
33. **Quardokus, E. M., N. Din, and Y. V. Brun.** 2001. Cell cycle and positional constraints on FtsZ localization and the initiation of cell division in *Caulobacter crescentus*. Mol. Microbiol. **39:**949–959.
34. **Quon, K. C., G. T. Marczynski, and L. Shapiro.** 1996. Cell cycle control by an essential bacterial two-component signal transduction protein. Cell **84:**83–93.
35. **Quon, K. C., B. Yang, I. J. Domian, L. Shapiro, and G. T. Marczynski.** 1998. Negative control of bacterial DNA replication by a cell cycle regulatory protein that binds at the chromosome origin. Proc. Natl. Acad. Sci. USA **95:**120–125.
36. **Roberts, R. C., C. Toochinda, M. Avedissian, R. L. Baldini, S. L. Gomes, and L. Shapiro.** 1996. Identification of a *Caulobacter crescentus* operon encoding *hrcA*, involved in negatively regulating heat-inducible transcription, and the chaperone gene *grpE*. J. Bacteriol. **178:**1829–1841.
37. **Ryan, K. R., E. M. Judd, and L. Shapiro.** 2002. The CtrA response regulator essential for Caulobacter crescentus cell-cycle progression requires a bipartite degradation signal for temporally controlled proteolysis. J. Mol. Biol. **324:**443–455.
38. **Sackett, M. J., A. J. Kelly, and Y. V. Brun.** 1998. Ordered expression of *ftsQA* and *ftsZ* during the *Caulobacter crescentus* cell cycle. Mol. Microbiol. **28:**421–434.
39. **Sambrook, J., E. F. Fritsch, and T. Maniatis.** 1989. Molecular cloning: a laboratory manual, 2nd ed. Cold Spring Harbor Laboratory Press, Cold Spring Harbor, N.Y.
40. **Sciochetti, S. A., T. Lane, N. Ohta, and A. Newton.** 2002. Protein sequences and cellular factors required for polar localization of a histidine kinase in *Caulobacter crescentus*. J. Bacteriol. **184:**6037–6049.
41. **Sciochetti, S. A., N. Ohta, and A. Newton.** 2005. The role of polar localization in the function of an essential Caulobacter crescentus tyrosine kinase. Mol. Microbiol. **56:**1467–1480.
42. **Simon, R., U. Prieffer, and A. Puhler.** 1983. A broad host range mobilization system for *in vivo* genetic engineering: transposon mutagenesis in gram-negative bacteria. Biotechnology **1:**784–790.
43. **Skerker, J. M., and L. Shapiro.** 2000. Identification and cell cycle control of a novel pilus system in Caulobacter crescentus. EMBO J. **19:**3223–3234.
44. **Sommer, J. M., and A. Newton.** 1991. Pseudoreversion analysis indicates a direct role of cell division genes in polar morphogenesis and differentiation in *Caulobacter crescentus*. Genetics **129:**623–630.
45. **Sommer, J. M., and A. Newton.** 1989. Turning off flagellum rotation requires the pleiotropic gene *pleD*: *pleA*, *pleC*, and *pleD* define two morphogenic pathways in *Caulobacter crescentus*. J. Bacteriol. **171:**392–401.
46. **Spratt, B. G., P. J. Hedge, S. te Heesen, A. Edelman, and J. K. Broome-Smith.** 1986. Kanamycin-resistant vectors that are analogues of plasmids pUC8, pUC9, pEMBL8 and pEMBL9. Gene **41:**337–342.
47. **Stephens, C., A. Reisenauer, R. Wright, and L. Shapiro.** 1996. A cell cycle-regulated bacterial DNA methyltransferase is essential for viability. Proc. Natl. Acad. Sci. USA **93:**1210–1214.
48. **West, L., D. Yang, and C. Stephens.** 2002. Use of the *Caulobacter crescentus* genome sequence to develop a method for systematic genetic mapping. J. Bacteriol. **184:**2155–2166.
49. **Wheeler, R. T., and L. Shapiro.** 1999. Differential localization of two histidine kinases controlling bacterial cell differentiation. Mol. Cell **4:**683–694.
50. **Wortinger, M., M. Sackett, and Y. Brun.** 2000. CtrA mediates a DNA replication checkpoint that prevents cell division in *Caulobacter crescentus*. EMBO J. **19:**4503–4512.
51. **Wu, J., N. Ohta, and A. Newton.** 1998. An essential, multicomponent signal transduction pathway required for cell cycle regulation in *Caulobacter*. Proc. Natl. Acad. Sci. USA **95:**1443–1448.
52. **Wu, J., N. Ohta, J. L. Zhao, and A. Newton.** 1999. A novel bacterial tyrosine kinase essential for cell division and differentiation. Proc. Natl. Acad. Sci. USA **96:**13068–13073.